EDN: GTRJTD
УДК 532.5.013.3

On One Exact Solution of an Evaporative Convection Problem with the Dirichlet Boundary Conditions

Victoria B. Bekezhanova*
Institute of Computational Modelling SB RAS
Krasnoyarsk, Russian Federation
Olga N. Goncharova†
Altai State University
Barnaul, Russian Federation

Received 16.10.2023, received in revised form 07.12.2023, accepted 08.01.2024

Abstract. Characteristics of steady-state convective flows of a liquid and a co-current gas flux under the conditions of inhomogeneous evaporation of the diffusive type in a flat horizontal channel are studied. A partially-invariant exact solution of equations of the thermosolutal convection is used to describe the flows within the framework of the Oberbeck – Boussinesq approximation. It is derived as the solution of the evaporative convection problem with the Dirichlet boundary conditions on the outer channel walls. The influence of the external thermal load on the structure of the velocity and temperature fields, evaporation mass flow rate and vapor content in the gas layer was investigated in the HFE-7100 – nitrogen system.

Keywords: mathematical model, boundary-value problem, exact solution, evaporative convection.

Citation: V.B. Bekezhanov, O.N. Goncharova, On One Exact Solution of an Evaporative Convection Problem with the Dirichlet Boundary Conditions, J. Sib. Fed. Univ. Math. Phys., 2024, 17(2), 207–219. EDN: GTRJTD.

Introduction

Traditional approach to describe the evaporative convection in two-phase systems is based on the use of the Navier–Stokes equations (or their approximations) supplemented by the heat transfer and molecular transport equations [1]. The set of governing relations for determining kinematic, temperature and concentration characteristics presents the thermosolutal convection equations. Due to the group properties the system of equation admits a partially invariant solution belonging to the Birikh class [2, 3]. Such type of solutions can be used for describing the evaporative convection in a bilayer liquid – gas system with a sharp interface in plane channels with solid impermeable walls in the frame of the two-sided approach [1]. Various well-posed statements of the boundary value problems for the thermosolutal convection equations were analysed [4, 5]. It was shown that the use of the Dirichlet boundary conditions for all the required functions on the external boundaries of the flow domain allows one to derive the informative Birikh type exact solution. It correctly takes into account the impact of the thermocapillary and thermodiffusion effects, non-uniform character of diffusion-limited evaporation on the phase

*vbek@icm.krasn.ru https://orcid.org/0000-0003-2068-6364
†gon@math.asu.ru https://orcid.org/0000-0002-9876-4177

boundary as well as the influence of the thermal load applied on the channel walls. It should be noted that non-constant evaporation rate along the liquid surface was fixed in physical experiments [6]. In the present paper, the mentioned above solution of the Dirichlet problem is used to study characteristics of gas sheared liquid flows in a horizontal channel under various intensity of the external thermal load. Applicability conditions of the exact solution to model steady-state convective flows of a liquid and a co-current gas flux are specified.

1. Statement of the problem and anzatz of solution

Let us consider the combined convection in a system of two viscous heat-conducting incompressible fluids (liquid and gas-vapour mixture) in a flat horizontal mini-channel with solid impermeable walls $y = -l$ and $y = h$ (Fig. 1). The two-phase system is in the terrestrial conditions with the vector of the gravity force acceleration $\mathbf{g} = (0, -g)$, $g = 9.81$ m/s^2. Basic characteristics of this system are the velocity $\mathbf{v}_i$, temperature T_i, pressure p_i of both media, and vapour concentration C in the gas. Here and below, the subscript or superscript $i = 1$ and $i = 2$ corresponds to the characteristics of the fluids in the lower and upper layers, respectively.

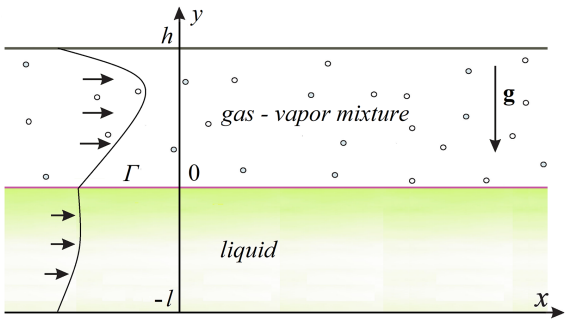

Fig. 1. The sketch of a two-phase system in the Cartesian coordinates

When posing the problem, the following assumptions are supposed to be satisfied.

(i) Surface between the liquid and gas phases is the thermocapillary interface Γ enabling the mass transfer due to evaporation/condensation. Only diffusive type evaporation occurs, and convective mass transfer through Γ is not considered. Here, the surface remains in the non-deformed state $y = 0$. The tangential forces, induced by the thermocapillary effect and shear stresses due to the gas pumping, act on Γ. The surface tension of the phase boundary is specified by the function $\sigma = \sigma_0 - \sigma_T(T - T_0)$, where σ_0, T_0 are the characteristic values of the surface tension and liquid temperature, respectively, σ_T is the temperature coefficient of surface tension.

(ii) The liquid volatilizes across the interface at a rate M so that the mixture of the carrier gas and liquid vapour fills the upper layer. Vapour is considered as a passive admixture. The Soret and Dufour effects appear in the gas phase due to presence of the volatile component.

(iii) The reference values T_0, p_0, C_0 characterize the thermodynamic equilibrium state of the two-phase system. The ground state of the system described by the above-mentioned basic functions is close to the thermodynamic equilibrium state or slightly deviates from it, i.e., convection under the Boussinesq conditions is considered.

(iv) Thermal load distributed according to the linear law with respect to the longitudinal coordinate is applied on channel walls.

Basic factors governing regimes of convective flows in the strip confined by fixed walls are the buoyancy force, the Marangoni effect, gas pumping and linear heating of the outer boundaries. To describe the stationary flows of each medium the Navier – Stokes equations in the Oberbeck – Boussinesq approximation are used:

$$\begin{gathered}\frac{\partial u}{\partial x}+\frac{\partial v}{\partial y}=0, \quad u\frac{\partial u}{\partial x}+v\frac{\partial u}{\partial y}=-\frac{1}{\rho_0}\frac{\partial p}{\partial x}+\nu\left(\frac{\partial^2 u}{\partial x^2}+\frac{\partial^2 u}{\partial y^2}\right),\\ u\frac{\partial v}{\partial x}+v\frac{\partial v}{\partial y}=-\frac{1}{\rho_0}\frac{\partial p}{\partial y}+\nu\left(\frac{\partial^2 v}{\partial x^2}+\frac{\partial^2 v}{\partial y^2}\right)+g\left(\beta T+\gamma C\right), \qquad (1.1)\\ u\frac{\partial T}{\partial x}+v\frac{\partial T}{\partial y}=\chi\left(\frac{\partial^2 T}{\partial x^2}+\frac{\partial^2 T}{\partial y^2}+\delta\left(\frac{\partial^2 C}{\partial x^2}+\frac{\partial^2 C}{\partial y^2}\right)\right).\end{gathered}$$

The vapour transfer in the background gas is governed by the convection-diffusion equation [7]:

$$u\frac{\partial C}{\partial x}+v\frac{\partial C}{\partial y}=D\left(\frac{\partial^2 C}{\partial x^2}+\frac{\partial^2 C}{\partial y^2}+\alpha\left(\frac{\partial^2 T}{\partial x^2}+\frac{\partial^2 T}{\partial y^2}\right)\right). \qquad (1.2)$$

Terms γC and $\delta\Delta C$ in the momentum and energy transport equations, respectively, as well as equation (1.2) are taken into account to model the flow in the upper gas layer only. The following notations are used: u, v are the projections of the velocity vector $\mathbf{v}$ on the Ox and Oy axes, p is the modified pressure, ρ_0 is the average fluid density, ν is the coefficient of kinematic viscosity, β is the thermal expansion coefficient, γ is the coefficient of concentration expansion, χ is the coefficient of heat diffusivity, D is the coefficient of vapour diffusion in the gas, and the coefficients δ and α characterize the diffusive thermal effect and the thermodiffusion effect in the gas-vapour layer, correspondingly. It is worth noting that within the frame of the Oberbeck – Boussinesq approximation function p describes deviation of the physical (true) fluid pressure P from the hydrostatic one. Taking into account the hydrostatic component and equilibrium characteristics of each fluid, one can obtain $p_i = P_i - \tilde{\rho}_i \mathbf{g}\cdot\mathbf{x}$. Here, $\tilde{\rho}_1 = \rho_{01}(1+\beta_1 T_0)$, $\rho_2 = \rho_{02}(1+\beta_2 T_0+\gamma C_0)$.

System of equations (1.1), (1.2) admits a stationary exact solution of the form

$$\begin{gathered}u_i = u_i(y), \quad v_i = 0, \quad T_i = T_i(x,y) = (a_1^i + a_2^i y)x + \vartheta_i(y),\\ C = C(x,y) = (b_1 + b_2 y)x + \phi(y), \quad p_i = p_i(x,y).\end{gathered} \qquad (1.3)$$

Here, a_j^i, b_j $(j = 1, 2)$ are parameters of the solution. They satisfy some compatibility relations dictated by the boundary conditions. Solution (1.3) as the solution of an evaporative convection problem was first proposed in [8]. Its treatment as the partially invariant exact solution of rank 1 and defect 3 was given in [2]. Below, conditions on the outer boundaries $y = -l$ and $y = h$ and on the internal interface $y = 0$ are formulated with regard to the solution form.

The Dirichlet boundary conditions are set on the channel walls for all required functions:

$$\begin{gathered}y = -l, \quad u_1 = 0, \quad T_1 = A_1 x + \vartheta_1,\\ y = h: \quad u_2 = 0, \quad T_2 = A_2 x + \vartheta_2, \quad C = 0.\end{gathered} \qquad (1.4)$$

Here, A_i are given constant longitudinal temperature gradients that determines intensity and type (heating or cooling) of the thermal load applied on the walls, ϑ_1, ϑ_2 are constants setting an average temperature of the wall. In the general case when $\vartheta_1 \neq \vartheta_2$, the transverse temperature drop is formed in the channel. Then, temperature field in the entire flow domain is characterized by resulting non-uniform gradient with respect to y. Relations for velocity functions present the

no-slip conditions. If vapour concentration is equal to zero then it is interpreted as the condition of full vapour absorption on the upper wall. For the first time this condition was considered in [8]. Later, it was tested in analogical problem within the frame of three-dimensional statement [9]. The comparison of modelling results with experimental data showed that the use of such type of condition allowed one to describe the influence of edge effects. The effects presents as significant growth of evaporation rate near the three-phase contact line [10]. Condition $C = 0$ can be realized in experiments by the vapour freezing.

The following conditions are to be satisfied on the common internal boundary Γ

$$\begin{aligned} &y = 0: \quad \rho_1\nu_1\frac{du_1}{dy} = \rho_2\nu_2\frac{du_2}{dy} - \sigma_T\frac{\partial T_1}{\partial x}, \quad p_1 = p_2, \\ &\kappa_1\frac{\partial T_1}{\partial y} - \kappa_2\frac{\partial T_2}{\partial y} - \delta\kappa_2\frac{\partial C}{\partial y} = -LM, \\ &u_1 = u_2 = u_\Gamma, \quad T_1 = T_2 = T_\Gamma, \quad C = C_0[1 + \varepsilon(T_2 - T_0)]. \end{aligned} \tag{1.5}$$

The first two expressions present projections of the dynamic condition on the unit tangential and normal vectors to Γ. The third condition is the heat balance relation when transfer through the interface takes place. The fourth and fifth equalities set the continuity conditions for the velocity and temperature. The last relation gives the concentration of saturated vapour. Taking into account the solution form and assumption on the diffusive character of evaporation, the kinematic condition is satisfied identically. The following notations are used in (1.5): κ is the heat conductivity coefficient, L is the latent heat of vaporization, u_Γ and T_Γ are common values of velocity and temperature on the interface, respectively, $\varepsilon = L\mu/(RT_0^2)$, μ is the molar mass of evaporating liquid, and R is the universal gas constant. The mass balance condition is used to evaluate evaporation rate M. In the present paper, the case when M is not constant is considered. It varies along the channel according to the linear law

$$M = -D\rho_2\Big(\frac{\partial C}{\partial y} + \alpha\frac{\partial T_2}{\partial y}\Big), \quad M = M(x) = M_0 + M_x x. \tag{1.6}$$

Positive values of M refer to evaporation of the liquid into the gas flux, and negative ones correspond to vapour condensation.

Additional condition that defines the gas flow rate in the upper layer closes the problem statement:

$$Q = \int_0^h \rho_2 u_2(y)\, dy. \tag{1.7}$$

Explicit expressions for all required functions derived in the frame of the problem statement under consideration are presented in [4]. Therein, the physical interpretation of exact solution (1.3) is given, and the domain of its applicability for describing two-phase flows in real physical systems is discussed. Complete analysis of the applicability conditions of this solution for all possible problem statement was carried out [5].

It should be noted that solution (1.3) can be derived without using any assumption about shape of the interface. The second equality in (1.5) can be considered as the first term of the expansion of the dynamical condition for the normal stresses with respect to small capillary number Ca. The structure of the exact solution dictates the rectilinear shape of the interface within the framework of the problem statement under study when the leading term of the expansion leads to zero mean curvature of the interface (for details see [9]). Experimental possibility to maintain the plane form of the phase boundary of an evaporating liquid layer blown by a gas flux was described in [11].

2. Calculation of the solution parameters characterizing temperature, evaporation rate and vapour content

Substituting required functions (1.3) in governing equations (1.1), (1.2), functional representations for velocity u_j, temperature T_j, pressure p_j and concentration C can be we found (see [4]). Constants M_0 and M_x that determine evaporation rate as well as solution parameters a_j^i, b_j satisfy relations based on the boundary conditions.

First of all parameters a_1^1 and a_1^2 are equal to each other, $a_1^i = A$ as it follows from the continuity condition for the temperature on the phase boundary. Therefore, temperature functions in the layers take the form $T_i = (A + a_2^i y)x + \vartheta_i(y)$. Here, A is the longitudinal temperature gradient on Γ that determines the intensity of the thermocapillary convection and evaporation process.

Conditions of linear temperature distribution on the rigid channel walls $y = -l$ and $y = h$ result in the following relations for a_2^i: $a_2^1 = (A - A_1)l^{-1}$, $a_2^2 = (A_2 - A)h^{-1}$.

Taking into account the condition of zero vapour concentration on the upper wall $y = h$, one can obtain the following equality that relates parameter b_1 to parameter b_2: $b_1 + b_2 h = 0$. The Clapeyron – Clausius equation in the linearised form gives the saturated vapour concentration on Γ (the last condition in (1.5)). The consequence of this equation entails relationship $b_1 = C_0 \varepsilon A$. Then, $b_2 = C_0 \varepsilon A/h$.

Further, the gradient of evaporative mass flow rate M_x can be directly calculated with the help of mass balance condition (1.6):

$$M_x = -D\rho_2\big(b_2 + \alpha a_2^2\big) = -D\rho_2 h^{-1}\big(- A(C_0\varepsilon - \alpha) + \alpha A_2\big), \tag{2.1}$$

whereas the relation for M_0 that defines the average value of evaporation rate contains integration constants included in expressions for temperature and concentration functions.

Using the heat transfer condition at the interface and expression (2.1), the following relationship between a_2^1 and a_2^2 is obtained

$$a_2^2 = K a_2^1 + \bar{K} M_x, \quad K = \frac{\kappa_1}{\kappa_2(1 - \alpha\delta)}, \quad \bar{K} = \frac{D\rho_2\lambda + \delta\kappa_2}{D\rho_2\kappa_2(1 - \alpha\delta)}.$$

Since a_2^1, a_2^2 and M_x depend on A, A_1, A_2, condition on constraint is

$$A_2\big(1 + \alpha D\rho_2\bar{K}\big) = A\big(1 + hl^{-1}K + (C_0\varepsilon + \alpha)D\rho_2\bar{K}\big) - A_1 hl^{-1}K. \tag{2.2}$$

Expression (2.2) establishes relation between longitudinal temperature gradients A, A_1 and A_2 on system boundaries. Two coefficients defining temperature gradients are prescribed arbitrarily; the third one is found according to (2.2). One should note that in a real physical system evaporation results in cooling of the liquid surface and formation of longitudinal temperature gradient at the interface. Thus, this gradient can be evaluated on the basis of the exact solution. According to (2.2), interfacial temperature gradient A depends on boundary gradients A_i, geometric parameters of the system and physical parameters of the fluids.

In view of the form of the exact solution, the vapour concentration function increases with x. Since function C is treated as mass fraction of the volatile component in the gas phase, it has a physical meaning only if its values belong to the interval $[0; 1]$. The extent of the flow domain L_h where C takes on feasible values can be determined in the terms of input data of the problem. According to the last condition in (1.5), changes in vapour content along the

longitudinal coordinate x can be evaluated as follows: $C \sim C_0(1 + \varepsilon A x)$. Then, the length L_h can be evaluated as follows $L_h \leqslant (1 - C_0)/\varepsilon A C_0$.

Below, the obtained solution of the Dirichlet problem is used to study the influence of the applied thermal load on the characteristics of flow regimes in two-phase systems.

3. Characteristics of convective regimes with non-uniform evaporation

********** Let us consider the bilayer system with HFE-7100 liquid and nitrogen gas as working media. Physical parameters of fluids are given in the order {HFE-7100, nitrogen} or only for one of the media: $\rho = \{1.5 \cdot 10^3,\ 1.2\}$ kg/m^3; $\nu = \{0.38 \cdot 10^{-6},\ 0.15 \cdot 10^{-4}\}$ m^2/s; $\beta = \{1.8 \cdot 10^{-3},\ 3.67 \cdot 10^{-3}\}$ K^{-1}; $\chi = \{0.4 \cdot 10^{-7},\ 0.3 \cdot 10^{-4}\}$ m^2/s; $\kappa = \{0.07,\ 0.027\}$ W/(m·K), $\sigma_T = 1.14 \cdot 10^{-4}$ N/(m·K), $\gamma = -0.5$, $D = 0.7 \cdot 10^{-5}$ m^2/s, $\alpha = 5 \cdot 10^{-3}$ K^{-1}, $\delta = 10^{-5}$ K, $L = 1.11 \cdot 10^5$ W·s/kg. The equilibrium characteristics of the bilayer system are $C_0 = 0.45$, $T_0 = 293.15$ K; here, $\varepsilon = 0.04$ K^{-1}, $\mu = 0.25$ kg/mol.

Velocity and temperature fields in the system, vapour content in the gas layer and evaporation rate that depend on the character and intensity of the thermal load applied on the external boundaries of the flow domain are analysed. Parameters defining the external thermal action are the longitudinal temperature gradients A_1, A_2 and ϑ_1, ϑ_2 (see (1.4)). Relation (2.2) is used to evaluate the interface gradient A at various boundary gradients A_i. Values of A_i vary from -10 to 10 K/m, and ϑ_1, ϑ_2 are equal to 293.15 K unless otherwise specified. If $A_i < 0$ ($A_i > 0$) then the channel wall is cooled (heated) in the direction of the longitudinal axes. For the working media used and heating conditions under consideration, the length L_h should be within 0.4 m. The thickness of the liquid layer $l = 0.0025$ m, the thickness of the gas layer $h = 0.005$ m and gas flow rate $Q = 9.6 \cdot 10^{-6}$ kg/(m^2·s) are fixed for all cases under consideration.

Influence of the longitudinal temperature gradient. One of the important factors that defines the pattern of the arising convective regime is the interface temperature gradient A. It is this parameter which governs the intensity of the surface tension-driven convection. Considering data listed in Tabs. 1, 2, one can conclude that interfacial gradient A and other parameters of the system are more sensitive to variations of boundary gradient A_1 then variations of A_2. In the tables, $\triangle T$ denotes the temperature drop in the whole system, $T_{\max}$ and $|u|_{\max}$ are the maximum values of the temperature and the absolut value of velocity in the system, respectively, $C_{\max}$ is the maximum value of the vapour concentration in the gas layer. In all considered cases the solution predicts relative variations of the temperature and deviations of maximum values of the vapour concentration from the equilibrium values T_0, C_0 retained within 15% which can be considered to be moderate ones.

Significant alterations in flow topology and thermal field occur with the change in A_i. When analysing basic characteristics of convective regimes, the Napolitano classification of flow types is used in the two-layer systems on the basis of the flow topology [12]. Three basic classes are distinguished: mixed type flows (MF), Poiseuille-type regimes (PF) and pure thermocapillary flows (TKF). Additionally, subclasses of MF and PF that are specific to two-phase systems with evaporation are considered. Detailed description of specific features and mechanisms causing all possible flow regimes as well as examples of velocity, temperature and vapour concentration fields for each mode can be found in [5]. The first form of mixed type flows (MF-1) is defined by the specific "negative lamination" of the velocity contour near the liquid – gas boundary and

Table 1. Parameters of the two-phase system at fixed $A_2 = 5$ K/m for different values of A_1

A_1, K/m	A, K/m	$\triangle T$, K	$T_{\max}$, K	$C_{\max}$	$\lvert u\rvert_{\max}\times$, $\times 10^{-3}$, m/s	$M_0 \cdot 10^4$, kg/(m^2·s)	$M_x \cdot 10^4$, kg/(m·s)
−10	−6.596	1.628	293.15	0.4216	2.423	6.9407	−2.909
−5	−2.875	2.097	293.15	0.4134	2.171	6.7669	−1.5049
0	0.846	2.23	293.15	0.4111	2.428	6.7193	−0.1008
5	4.567	2.024	293.15	0.4147	2.78	6.798	1.3034
10	8.289	1.482	293.15	0.4241	3.164	7.0028	2.7075

Table 2. Parameters of the two-phase system at fixed $A_1 = 5$ K/m for different values of A_2

A_2, K/m	A, K/m	$\triangle T$, K	$T_{\max}$, K	$C_{\max}$	$\lvert u\rvert_{\max}\times$, $\times 10^{-3}$, m/s	$M_0 \cdot 10^4$, kg/(m^2·s)	$M_x \cdot 10^4$, kg/(m·s)
−10	2.029	2.204	293.15	0.4115	2.51	6.7295	1.6056
−5	2.875	2.158	293.15	0.4123	2.598	6.7468	1.5049
0	3.721	2.098	293.15	0.4134	2.688	6.7697	1.4041
5	4.567	2.024	293.15	0.4147	2.78	6.798	1.3034
10	5.413	1.935	293.15	0.4162	2.873	6.8317	1.2026

formation of near-surface reverse flow (Fig. 2(a–c)). The second type mixed flow (MF-2) is characterized by the "positive stratification" of the velocity profile along the interface. Here, the longitudinal velocity component is positive in both fluids (Fig. 2(d–f)). Mixed flows of the third type (MF-3) have the velocity field similar to the Couette structure in one of the layers (Fig. 2(g–i)) or concurrently in both layers. It was found that all three classes of mixed type flows could be realized in the system under considered conditions.

In the general case, three subclasses of flows among the Poiseuille-type regimes were identified [5]. However, in the considered range of boundary gradients A_i, one can observe only flows with the velocity distribution close to the parabolic one through the whole height of the channel or simultaneously in both phases, where the longitudinal velocity component is positive everywhere. Such a flow regime presents the PF-1 regime (Fig. 3(a–c)). Finally, pure thermocapillary flows (TKF, Fig. 3(d–f)) which are characterized by global liquid counterflow can be also realized in the two-phase system under conditions of temperature pumping with gradients A_i from the specified range. Several consecutive transitions from one type of flows to another can occur with an increase in A_i from −10 to 10 K/m. Topological regimes arising in the bilayer system under study are specified on the map of flow regimes in Fig. 4(a) according to the given classification. Along with the topology of the flow, the intensity of the motion also varies. It is characterized by maximum values of the modulus of velocity $|u|$ (see Tabs. 1, 2) and it can be varied by more than 40%. As previously mentioned, the system is less sensitive to variations in A_2. When A_2 is changed from −10 K/m to 10 K/m, a smaller number of successive transitions between regimes is observed in comparison with corresponding variations in A_1. The intensity of the flow slightly responds to changes in the thermal load caused by variations in A_2 (compare values of $|u|_{\max}$ in Tabs. 1 and 2). One should note that all three basic types of flows are observed in real systems with evaporating liquid driven by the co-current gas flux [13].

The change of intensity of temperature driving forces leads not only to transformation of the velocity field but also to alteration of the thermal picture. The solution predicts formation of the non-uniform temperature gradient in the vertical direction for all observed convective regimes.

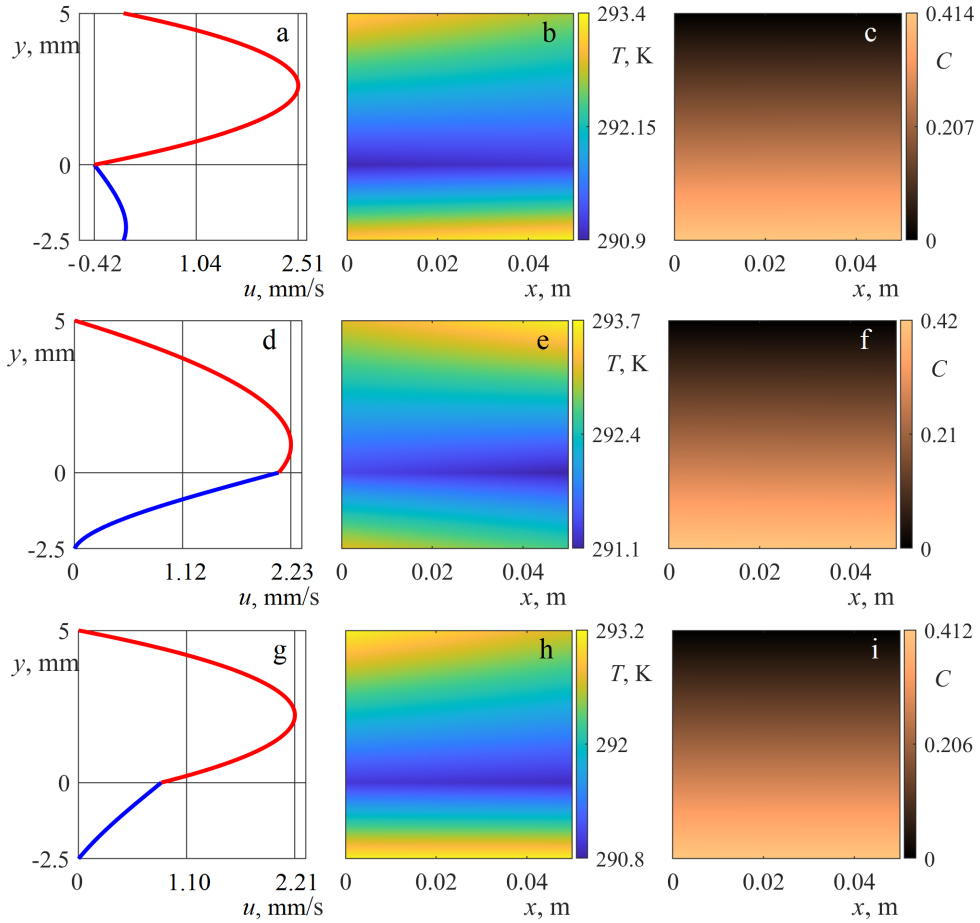

Fig. 2. Velocity (a, d, g), temperature (b, e, h) and vapour concentration (c, f, i) fields for mixed type flows: MF-1, $A_1 = 5$ K/m, $A_2 = -10$ K/m (a–c); MF-2, $A_1 = -10$ K/m, $A_2 = 10$ K/m (d–f); MF-3, $A_1 = 0$ K/m, $A_2 = -10$ K/m (g–i)

Two typical thermal patterns with a substantial "cold" zone on both sides of the phase boundary (CNsZ) and with a cold thermocline along the interface (CThI) can emerge. The regimes with the cool near-surface zone (CNsZ) are characterized by unstable temperature stratification of the entire liquid layer. In this case, the gas layer is steadily stratified (Figs. 2(b, e, h), 3(b)). The evaporation effect prevails over the thermocapillary effect in these modes. Formation of the distinctive cold thermocline on the interface (CThI) is caused by the competition of the Marangoni effect which gives rise to the thermocapillary motion of the liquid from the region with higher temperature into the cool domain along the interface with the evaporation process resulting in cooling of the liquid surface (Fig. 3(e)). The possibility of formation of convective modes with the cool boundary layer near the liquid surface in the two-layer systems with evaporation was confirmed in experiments [14]. Figure 4(b) presents a "map" of thermal regimes that depend on the longitudinal temperature gradients A_i.

The pattern of the vapour concentration field in the gas layer remains the same for all considered cases (see distributions of the vapour concentration functions in Figs. 2, 3). The vapour

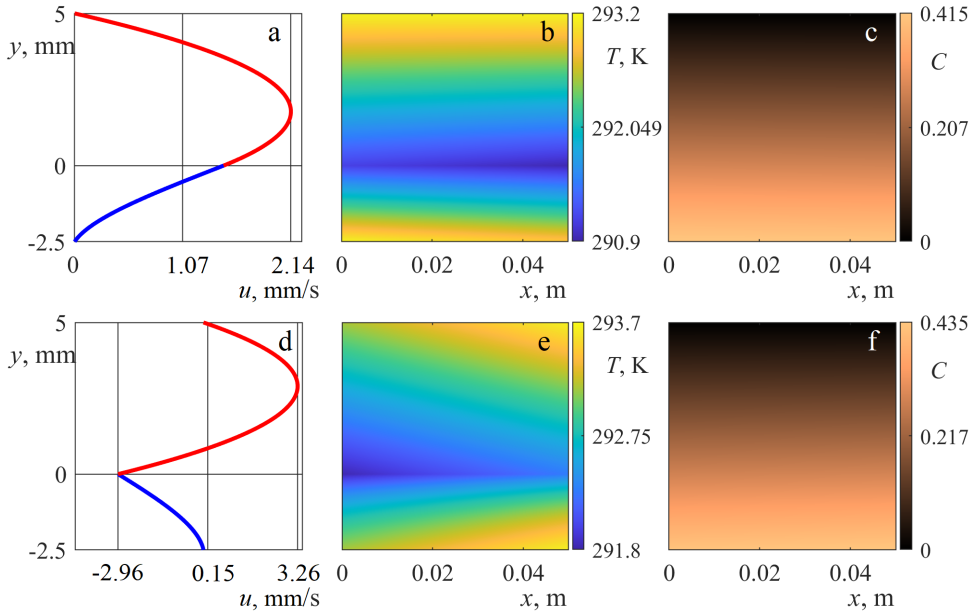

Fig. 3. Velocity (a, d), temperature (b, e) and vapour concentration (c, f) fields: PF-1, $A_1 = -5$ K/m, $A_2 = 0$ K/m (a–c); TKF, $A_1 = A_2 = 10$ K/m (d–f)

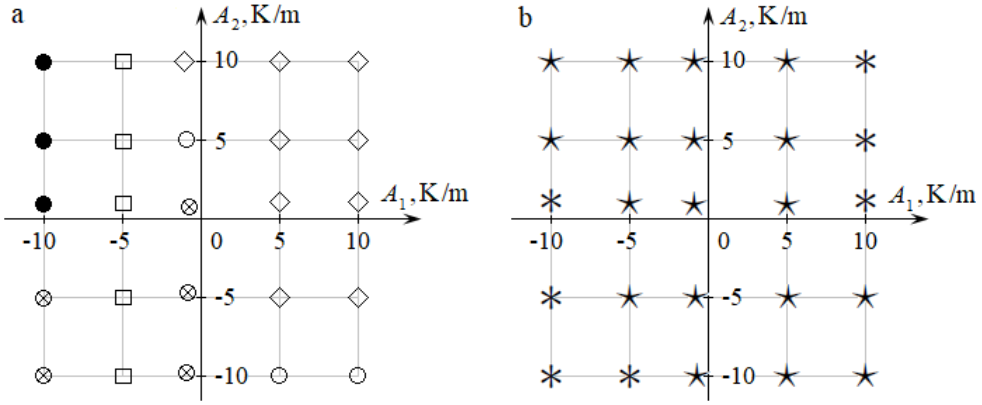

Fig. 4. Maps of flow regimes (a) and temperature patterns (b) in the HFE-7100–nitrogen system subjected to external thermal load: (a) — ○ – MF-1, ● – MF-2, ⊗ – MF-3, □ – PF-1, ◇ – TKF; (b) — ★ – regime with CNsZ, ∗ –regime with CThI

content is close to the concentration of saturated vapour C_0 near the interface, and it varies here depending on changes in the interfacial temperature gradient A whereas near the upper wall the values of C drop to zero. The behaviour of the vapour concentration function is caused by changes in the evaporation mass flow rate M which significantly depends on temperature characteristics of the interface. Since temperature gradient A is more sensitive to variations of the thermal load applied to the substrate then similar behaviour is inherent to M (compare the variation range for M_0, M_x in Tabs. 1, 2 and the character of their relation with changes in A

related to changes in boundary temperature gradients A_i presented in Fig. 5). If M_x is negative then the evaporation rate M decreases along the channel and the vapour concentration in the gas diminishes (Tab. 1). The higher is the temperature, the higher is the saturation pressure on the gas side of the phase interface. Therefore, more liquid evaporates at the same gas pressure. If the surface tension-driven motion is co-directional with the gas flow then evaporation is induced by both the thermal load and the effect associated with the shear stress. The gas flux encourages the vapour motion in the gas. It results in higher concentration gradient at the liquid – gas interface and ensures higher evaporation rate.

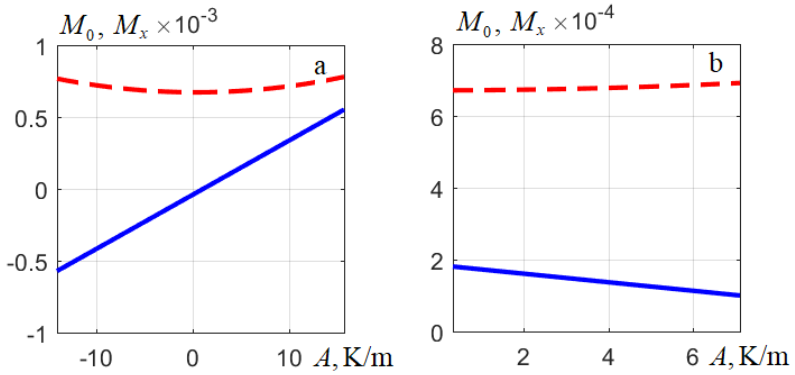

Fig. 5. Relationship between parameters M_0 (dashed lines) and M_x (solid curves) and interface temperature gradient with changes in A_1 (a) and A_2 (b): $A_2 = 20$ K/m; $A_1 = 20$ K/m

Thus, one can exert control over the evaporation rate and flow regimes with the intensity of thermal pumping defined by boundary gradients A_i. If it is necessary to retain the given temperature head on one of the walls then one can maintain acceptable variations of the evaporation rate by means of the thermal regime on other wall and forecast potential changes in the vapour content.

Influence of the vertical temperature gradient. The structure of the thermal field can be considerably transformed with conditions of thermal load with non-zero gradients A_i and various ϑ_1 and ϑ_2. It depends on the value and orientation of the resulting temperature gradient. Since the system behaviour is more responsive to variations of the thermal load applied on the substrate the influence of the vertical temperature drop on the bilayer flow characteristics is investigated when parameter ϑ_1 varies from 288.15 to 298.15 K. Formation of regimes with stable (Fig. 6(b)) and unstable (Fig. 6(e)) temperature stratification is studied in the transverse direction of the whole system. One should note that solution predicts only reconstruction of the thermal field whereas the velocity profile is not transformed with the changes in ϑ_1. According to (2.2) and (1.6), both interface temperature gradient A and gradient M_x defining the variation rate of M along the longitudinal axes do not depend on ϑ_1. It remains the same for corresponding fixed values of A_i for all vertical temperature drops (quantitative characteristics for configurations under consideration are exemplified in Tab. 3). It is regarded as a imperfection of solution (1.3) as in this case the exact solution does not reflect the impact of the Marangoni effect. One can conclude that the presence of non-zero transverse temperature drop does not lead to the formation of topologically new classes of flows that differ from those described earlier and presented in Figs. 2, 3.

Table 3. Parameters of the two-phase system at $A_1 = -5$ K/m, $A_2 = 5$ K/m with changes in ϑ_1

ϑ_1, K	$\triangle T$, K	$T_{\max}$, K	$C_{\max}$	$\lvert u\rvert_{\max}\times$, $\times 10^{-3}$, m/s	$M_0 \cdot 10^4$, kg/(m^2·s)	$M_x \cdot 10^4$, kg/(m·s)
288.15	5.818	293.15	0.3484	2.171	5.3628	−1.5049
293.15	2.097	293.15	0.4134	2.171	6.7669	−1.5049
298.15	5	298.15	0.4784	2.171	8.171	−1.5049

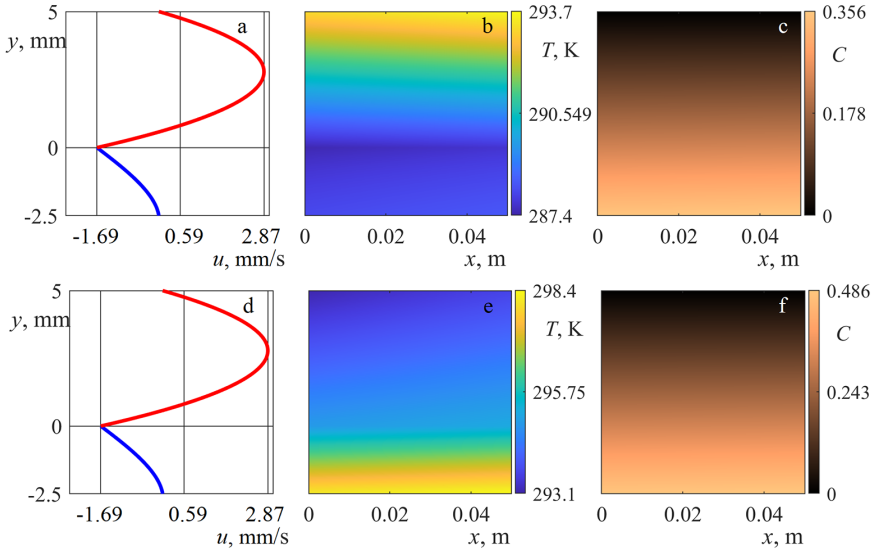

Fig. 6. Velocity (a, d), temperature (b, e) and vapour concentration (c, f) fields in the bilayer system at $A_1 = 5$ K/m, $A_2 = 10$ K/m for $\vartheta_1 = 288.15$ K (a–c) and $\vartheta_1 = 298.15$ K (d–f)

Despite the mentioned above defect this solution feasibly describes the qualitative interrelation of the variations of the evaporative mass flow rate and the vapour content in the gas with changes in the vertical temperature drop. The growth of deviation of the liquid temperature from the equilibrium value T_0 and significant deviation of vapour concentration in the gas phase from C_0 with an increase in the transverse temperature drop is observed. If $\vartheta_1 < T_0$ then the vapour content in the gas drops. The lower is the temperature of the liquid the lower is the average kinetic energy of the liquid volume and, therefore, the smaller is the quantity of the volatilizing fluid. Along with this, the lower is the vapour concentration in the background gas, the faster is the volatilization from the liquid phase [15]. With the rising temperature the average kinetic energy of the liquid volume increases. Therefore, vapour concentration C also grows accompanied by the inhibition of growth of the vaporization rate M. If $\vartheta_1 > T_0$ then the maximum vapour concentration is above the equilibrium concentration C_0. The solution precisely specifies this relationship between evaporation rate and characteristics of the vapour content in the gas phase and temperature drop in the whole system. Thus, the qualitative behaviour of evaporation characteristics that depends on the transverse temperature drop in the bilayer system is adequately described by the exact solution under study.

The applicability of solution (1.3) that describes characteristics of the bilayer system with the transverse temperature drop is limited by values of ϑ_1 and ϑ_2 providing moderate deviations of

$C_{\max}$ from C_0, namely, no more than 20–25%. For the considered two-layer system the transverse temperature drop should be within 10 degrees, where the average temperature of duct walls ϑ_1 and ϑ_2 have to be close to the temperature of the local thermodynamic equilibrium T_0.

The work of O. N. Goncharova was carried out in accordance with the State Assignment of the Russian Ministry of Science and Higher Education entitled "Modern methods of hydrodynamics for environmental management, industrial systems and polar mechanics" (Government contract code FZMW-2020-0008).

References

[1] V.B.Bekezhanova, O.N.Goncharova, Problems of the evaporative convection (review), *Fluid Dyn.*, **53**(2018), suppl. 1, S69-S102.

[2] V.K.Andreev, The Birikh Solution of Convection Equations and Some Its Generalization, Preprint no. 1-10, ICM SB RAS, Krasnoyarsk, 2010 (in Russian).

[3] V.V.Pukhnachev, Group-theoretical methods in convection theory, *AIP Conf. Proc.*, **1404**(2011), 27–38. DOI: 10.1063/1.3659901

[4] V.B.Bekezhanova, O.N.Goncharova, I.A.Shefer, Solution of a two-layer flow problem with inhomogeneous evaporation ate the thermocapillary interface, *J. Sib. Fed. Univ. Math. Phys.*, **14**(2021), no. 4, 404–413. DOI: 10.17516/1997-1397-2021-14-4-404-413

[5] V.B.Bekezhanova, O.N.Goncharova, Comparative characteristic of evaporative convection regimes in different statements of boundary value problem for convection equations, *J. Math. Sci.*, **267**(2022), no. 4, 444–456. DOI:10.1007/s10958-022-06149-4

[6] Y.V.Lyulin et al., The effect of the interface length on the evaporation rate of a horizontal liquid layer under a gas flow, *Thermophys. Aeromech.*, **27**(2020), no. 1, 117–121. DOI: 10.1134/S0869864320010114

[7] L.D.Landau, E.M.Lifshitz, Course of Theoretical Physics, Vol. 6, Fluid Mechanics, second ed., ButterworthHeinemahh, 1987.

[8] M.I.Shliomis, V.I.Yakushin, Convection in a two-layers binary system with an evaporation, *Collected papers: Uchenye zapiski Permskogo Gosuniversiteta, seriya Gidrodinamika*, **4**(1972), 129–140 (in Russian).

[9] V.B.Bekezhanova, O.N.Goncharova, Modeling of three dimensional thermocapillary flows with evaporation at the interface based on the solutions of a special type of the convection equations, *Applied Mathematical Modelling*, **62**(2018), 145–162. DOI: 10.1016/j.apm.2018.05.021

[10] V.S.Ajaev, O.A.Kabov. Heat and mass transfer near contact lines on heated surfaces, *Int. J. Heat Mass Transf.*, **108**(2017), 918–932. DOI: 10.1016/j.ijheatmasstransfer.2016.11.079

[11] Yu.Lyulin, O.A.Kabov. Thermal effect in the evaporation process from the interface of the horizontal liquid layer under ashear gas flow, *Interfacial Phenom. Heat Transf.*, **11**(2023), no. 1, 55–64. DOI: 10.1615/InterfacPhenomHeatTransfer.2023046985

[12] L.G.Napolitano, Plane Marangoni – Poiseuille flow two immiscible fluids, *Acta Astronaut.*, **7**(1980), 461–478.

[13] Yu.Lyulin, O.Kabov, Evaporative convection in a horizontal liquid layer under shear-stress gas flow, *Int. J. Heat Mass Transfer*, **70**(2014), 599–609.
DOI: 10.1016/j.ijheatmasstransfer.2013.11.039

[14] V.P Reutov et al., Convective structures in a thin layer of an evaporating liquid under an airflow, *J. Appl. Mech. Techn. Phys.*, **48**(2007), no. 4, 469–478.
DOI: 10.1007/s10808-007-0059-y

[15] P.I.Voropai, A.A.Shlepov, Enhancement of Reliability and Efficiency of Reciprocating Compressors, Nedra, Moscow, 1980 (in Russian).

Об одном точном решении задачи испарительной конвекции с граничными условиями Дирихле

Виктория Б. Бекежанова
Институт вычислительного моделирования СО РАН
Красноярск, Российская Федерация
Ольга Н. Гончарова
Алтайский государственный университет
Барнаул, Российская Федерация

Аннотация. Изучаются характеристики стационарных конвективных течений жидкости и спутного потока газа в плоском горизонтальном канале в условиях неоднородного испарения диффузионного типа. Для описания течений в рамках приближения Обербека – Буссинеска используется частично-инвариантное точное решение уравнений термоконцентрационной конвекции, полученное как решение задачи испарительной конвекции с граничными условиями Дирихле на внешних стенках канала. На примере системы сред HFE-7100 – азот исследовано влияние внешней тепловой нагрузки на структуру полей скорости и температуры, массовый расход испарения и паросодержание в газе.

Ключевые слова: математическая модель, краевая задача, точное решение, испарительная конвекция.